Preprints (www.preprints.org) | NOT PEER-REVIEWED | Posted: 29 September 2019 doi:10.20944/preprints201909.0324.v1

Peer-reviewed version available at Biomolecules 2019, 9, 651; doi:10.3390/biom9110651

Article

Immunotherapy of Hepatocellular Carcinoma with Magnetic PD-1 Peptide-imprinted Polymer Nanocomposite and Natural Killer Cells

Mei-Hwa Lee[1,†], Kaihsi Liu[2,†], James L. Thomas[3], Jyun-Ren Chen[4] and Hung-Yin Lin[4,*]

[1] Department of Materials Science and Engineering, I-Shou University, Kaohsiung 84001, Taiwan; meihwalee@ntu.edu.tw

[2] Department of Internal Medicine, Division of Cardiology, Zuoying Branch of Kaohsiung Armed Forces General Hospital, Kaohsiung 813, Taiwan; liukaihsi@gmail.com

[3] Department of Physics and Astronomy, University of New Mexico, Albuquerque, NM 87131, USA; jthomas@unm.edu

[4] Department of Chemical and Materials Engineering, National University of Kaohsiung, Kaohsiung 81148, Taiwan; linhy@ntu.edu.tw

[†] These authors contributed equally to the work.

*Correspondence: linhy@ntu.edu.tw; Tel.: + (O) +886(7)591-9455; (M) +886(912)178-751

Abstract: Programmed cell death protein 1 (PD-1) is a biomarker on the surface of cells that has a role in promoting self-tolerance by suppressing the inflammatory activity of T cells. In this work, one peptide of PD-1 was used as the template in molecular imprinting. The magnetic peptide-imprinted poly(ethylene-co-vinyl alcohol) composite nanoparticles (MPIP NPs) were characterized by dynamic light scattering (DLS), high-performance liquid chromatography (HPLC), Brunauer-Emmett-Teller (BET) analysis and superconducting quantum interference device (SQUID) analysis. Natural killer-92 (NK-92) cells were added to these composite nanoparticles and then incubated with human hepatoma (HepG2) cells. The viability and apoptosis pathway of HepG2 were then studied using cell counting kit-8 (CCK8) and the quantitative real-time polymerase chain reaction (qRT-PCR), respectively. These nanoparticles were found significantly enhance the activity of natural killer cells toward HepG2 cells by increasing expression of NK- B, caspase 8 and especially caspase 3.

Keywords: Immunotherapy; Human Hepatoma Cells; Programmed cell death protein 1 (PD-1); Magnetic nanoparticles; Peptide-imprinted Polymer; Natural Killer Cells.

1. Introduction

Programmed cell death protein 1 (PD-1), which was discovered by Tasuku Honjo in 1992,[1] is expressed on the surface of T-cells and plays a role in promoting self-tolerance of those cells by suppressing their inflammatory activity. The clinical use of PD-1 as a target in the treatment of patients with several types of cancer began in 2012.[2-3] The cancers thus treated included lung cancer, renal cancer, lymphoma and melanoma, as reviewed by Guan *et al.*[3] Trials of this treatment against these cancers have used checkpoint therapy with various targets on the cellular surface, such as cytotoxic-lymphocyte antigen-4 (CTLA-4) and programmed cell death protein-1 or its ligand (PD-1/L1).[3] Many anti-PD-1 and anti-PD-L1 agents have been developed and some of them (such as pembrolizumab, novolumab and atezolizumab)[3] have been approved by the Food and Drug Administration (FDA). Combination therapies, such as (anti-PD-1/anti-PD-L1)[4] or (anti-CTLA-4/ anti-PD-1)[5] have also undergone human trials.

© 2019 by the author(s). Distributed under a Creative Commons CC BY license.

Preprints (www.preprints.org) | NOT PEER-REVIEWED | Posted: 29 September 2019 doi:10.20944/preprints201909.0324.v1

Peer-reviewed version available at Biomolecules 2019, 9, 651; doi:10.3390/biom9110651

Hepatocellular carcinoma (HCC) is a leading cause of cancer-related morbidity and mortality,[6] especially in Asia. The immunological landscape and immunotherapy for HCC, which have been reviewed by Prieto *et al.*,[7] suggest that novel treatment methods are urgently needed. In HCC, the liver is enriched with various innate immune cells,[8] among which natural killer (NK) cells are important in host defense and maintaining immune balance.[9] Liver NK cells can produce IFN- and TNF- following the recognition by an NKG2D receptor.[10] NK cells contribute to immunotherapy that is mediated by a PD-1/PD-L1 blockade.[11] Four clinical trials in which the NK-92 cell line is used, rather than blood NK cells, have been reported upon.[12]

In 2007, Langer's group reported on nanocarriers as an emerging platform for cancer therapy.[13] Nanocarriers are typically liposomes, inorganic particles, metallic shells, amphipathic molecules, dendrimers or carbon nanotubes; these may incorporate biodegradable polymers / chemotherapeutics / surface functionalities / spacer groups / agents to promote a long circulation time, and targeting molecules (aptamers, antibodies or their fragments).[13] The safer delivery[14] harnessing design of nanoparticles[15] and their applications[16] in cancer therapy were extensively reviewed, including molecularly-targeted immunotherapy, nanoparticle delivery of immunotherapy agents, systemic gene delivery of immunomodulators to tumors, and using immune cells as drug carriers or targeting immunotherapy to immune cells.[14]

Molecularly imprinted polymers (MIPs) are synthesized with cavities with size and structure complementary to the template molecules. Upon removal of template, they can be used as artificial antibodies.[17] Conventionally, the template molecule that is used in the imprinting of proteins is the whole protein, to provide high selectivity and sensitivity. Potential disadvantages of whole protein templates include solubility limitations and price[18] for the preparation of MIPs. Therefore, some proteins such as albumin,[19] lysozyme[20] or hemoglobin have been employed as the model systems. Recently, peptide epitopes of proteins have been found by molecular simulation[21] or empirical methods,[22] and used as templates in molecular imprinting. Peptide-imprinted polymers have been characterized and found to achieve both high capacity and selectivity.[22] Peptides that contain six to 14 amino acids are typically selected as epitope templates for imprinting.[21] However, there are no general rules for peptide selection that involve the various functions of proteins, including catalysis, cell signaling and ligand binding, and protein structure.

Finding epitopes for enzymes, cell signaling and ligand binding proteins, and structural proteins may involve different considerations, such as the active sites of the enzymes, or the exposed structures of the ligand binding or structural proteins. Also, the solubility and interfacial properties of epitopes are important in the preparation of MIP nanoparticles (NPs).[19, 23] Our previous work has demonstrated not only the preparation but also the characterization of MIPs and their cancer-related application.[24-25] For example, a small molecule (orcinol) was templated onto MIP NPs for the extraction of an important bioactive molecule (resveratrol) from Chinese herb extract for the oral cancer cell treatments;[24] and a thymine-imprinted polymeric NP was used to promote the expression of p53 in the hepatoma cells.[25] In this work, the peptide derived from PD-1 was identified for molecular imprinting. Magnetic peptide-imprinted polymer nanoparticles (MPIP NPs) were formed by the phase separation of EVAL, and then characterized by dynamic light scattering (DLS) and surface area analysis. The isothermal adsorption and capacity of MPIP NPs were measured using HPLC. Finally, hepatoma (HepG2) cells were treated with PIP NPs and natural killer (NK-92) cells. The immune pathway of the HepG2 cells with PIP NPs was investigated using the quantitative reverse transcription-polymerase chain reaction (qRT-PCR).

2. Materials and Methods

2.1 Reagents.

Peptides AISLHPKAKIEES (Peptide A) of mPD-1 was ordered from Yao-Hong Biotechnology Inc. (HPLC grade, New Taipei City, Taiwan). Poly(ethylene-*co*-vinyl alcohol), EVAL, with ethylene 27, 32, 38 and 44 mol% (product no. 414077, 414093, 414085, 414107) and RT-PCR primers were from Sigma-Aldrich Co. (St. Louis, MO). Iron(III) chloride 6-hydrate (97%), iron(II) sulphate 7-hydrate

Preprints (www.preprints.org) | NOT PEER-REVIEWED | Posted: 29 September 2019 doi:10.20944/preprints201909.0324.v1

Peer-reviewed version available at Biomolecules 2019, 9, 651; doi:10.3390/biom9110651

(99.0%) and dimethyl sulfoxide (DMSO, product # 161954) were from Panreac (Barcelona, Spain). DMSO was used as the solvent to dissolve EVAL polymer particles in the concentration of 1 wt%. Absolute ethyl alcohol was from J. T. Baker (ACS grade, NJ). All chemicals were used as received unless otherwise mentioned.

2.2 Synthesis and formation of magnetic molecularly imprinted polymer composite nanoparticles

The synthesis of magnetic peptide-imprinted EVAL composite nanoparticles (MPIP NPs) including the following steps. Magnetic nanoparticles, synthesized by co-precipitation of a mixture of iron (III) chloride 6-hydrate and iron (II) sulphate 7-hydrate by sodium hydroxide, were repeatedly washed while adsorbed on a magnetic plate. The magnetic nanoparticles were washed three times with deionized water, and then to make them dispersed using ultrasonic for 30 s. In Scheme 1, peptide was dissolved in appropriate deionized water, the concentrations of peptide were 0.2, 2, 20, 100 and 200 μg/mL. The 250 μL DMSO solution was added into the same volume of peptide solution to form clear EVAL solution, and 10 mg of those composite particles were then added. The dispersion of 0.5 mL EVAL solution in 10 mL deionized water; and then removal of the template molecule by washing in 10 mL deionized water 15 mins for three times, separating the MPIPs magnetically after each washing. The non-imprinted polymers (NIPs) were prepared identically without peptide addition.

2.3 Characterization of magnetic molecularly imprinted polymer composite nanoparticles

Magnetic (MNP), peptide- (MPIP) and non-imprinted (MNIP) EVAL composite particles were monitored by a particle sizer (90Plus, Brookhaven Instruments Co., NY). The dynamic light scattering (DLS) measurement of the particle size distribution was at 25°C with 3 min duration data collection at the 90° detection angle. The magnetization of magnetic, peptide-imprinted polymers nanoparticles before and after template removal was monitored with a magnetic property measurement MPMS XL-7 system (Quantum Design, San Diego, CA) at 298 K in ±15000 Gauss.

The adsorption of peptide on nanoparticles was examined with a high-pressure liquid chromatography (HPLC) system. Peptide solution (1 mg/mL) in water was diluted to various concentrations for calibration. The solutions were passed through a 0.22 m PVDF syringe filter (Advangene Consumables Inc., USA) and then injected to a high-pressure liquid chromatography (HPLC) system for analysis of peptide. The separation was performed on a Kromasil 100-5 C18 column (5 μm particle size, pore size 100 Å, 25 cm x 4.6 mm I.D., Sigma-Aldrich, USA). The sample (20 μL) was eluted with a mobile phase composed of 0.1% TFA in 100% water (solvent A) and 0.1% TFA in 100% acetonitrile (solvent B). The gradient profile of peptide A is following below: 0-0.1 min, 12% A, 88% B; 0.1-25 min, 37% A, 63% B; 25.01-30 min, A 100%. The flow rate and detection wavelength were set to be 1.0 mL/min and 220 nm, respectively. The retention time is 6.19 min for peptide A.

2.4 Cytotoxicity test of HepG2 cells with magnetic molecularly imprinted composite nanoparticles and NK-92 cells.

2.4.1 MTT assay

HepG2 (Human hepatoblastoma cells, BCRC # 60364) cells were cultured in 90% of a 1:1 ration mixture of Dulbecco's modified Eagle's medium (DMEM) and Ham's F12 medium with 10% heat-inactivated FBS (fetal bovine serum), supplemented with 0.4 mg/mL G418 (Geneticin) at 37°C and 5% CO_2. For the cytotoxicity experiments about 10 μL of $7.5.0x10^4$ HepG2 cells and 190 μL culture medium per well ($7.5 x10^3$ HepG2 cells per well) were seeded in 96 well culture plates and then incubated f at 37 °C in 5% CO_2 for 24 h. Various concentrations of nanoparticles were added to each well at 37 °C for 24 h. Twenty microliters MTT (3-(4,5-dimethylthiazol-2-yl)-2,5diphenyltetrazolium bromide, a yellow tetrazole) solution in phosphate buffered saline (PBS) was added to each well after 24 h, and then incubated in 5% CO_2 for 3 h at 37 °C. The solution was removed from each well. Then, 100 μL dimethyl sulfoxide (DMSO) was added in each well and incubated at 37 °C for 30 min in the dark. The absorbance of this colored solution can be quantified at a measuring wavelength of 570nm

Preprints (www.preprints.org) | NOT PEER-REVIEWED | Posted: 29 September 2019 doi:10.20944/preprints201909.0324.v1

Peer-reviewed version available at Biomolecules 2019, 9, 651; doi:10.3390/biom9110651

against 620 nm as reference by a ELISA reader (CLARIOstar Reader, BMG Labtech, Offenburg, Germany). Effective adsorption is defined as the subtraction of the absorption from the emission to reference wavelengths. The percentage of cell viability was calculated as the number of viable cells divided by the total from the ratio of effective absorption of experimental cells to controls. Experiments were carried out in quadruplicate wells and repeated at least three times.

2.4.2 Cell Counting Kit-8 (CCK-8)- WST-8 Cell Proliferation Cytotoxicity Assay

NK-92 (Human natural killer cell, BCRC # 60414) cells were cultured in RPMI1640with L-glutamine and 10% FBS at 37°C and 5% CO_2. The CCK-8 test (Sigma-Aldrich Chemical Co., USA) is used as a rapid and sensitive method for toxicity of MNIPs, MNIPs with NK-92 cells and MPIPs with NK-92 cells. 200 µL of 5.0x10^5 HepG2 cells and 1.8 mL culture medium per well (5 x10^4 HepG2 cells/well) were seeded in 24 well culture plates and then incubated at 37 °C in 5% CO_2 for 24 h. The synthesized MNIPs or MPIPs composite nanoparticles were mixed with NK-92 cells medium for 10 minutes as shown in Scheme 1. NK-92 cells with NIPs or MPIPs 0.5 mL were added into HepG2 cells, and incubated at 37 °C in 5% CO_2 for 24 hr. Particles were removed from wells and 500 L of CCk-8 solution was added before ELISA measurements. The absorption intensities were measured by an ELISA reader (CLARIOstar, BMG Labtech, Offenburg, Germany) for the wavelength at 450 nm (I_{450}), and the reference absorption (I_{ref}, to account for turbidity and scattering) was obtained at the wavelength of 650 nm. The cellular viability (%) was then calculated from the ratio of effective absorption (I_{450}-I_{ref}) of experimental cells to controls. CCk-8 solutions were removed and added the 2 mL medium to each well for the next round of cellular viability test.

2.5 Gene expression of HepG2 cells treated with molecularly imprinted polymer composite nanoparticles.

The sequence (5′- 3′) of primers for NF-κβ1, Caspase 8, Caspase 3, GAPDH genes were: NF-κβ1, Forward: CACAAGGAGACATGAAACAG; Reverse: CCATGACAGCAAATCTCC. Caspase 8, Forward: CTACAGGGTCATGCTCTATC; Reverse: ATTTGGAGATTTCCTCTTGC. Caspase 3, Forward: AAAGCACTGGAATGACATC; Reverse: CGCATCAATTCCACAATTTC. GAPDH, Forward: ACAGTTGCCATGTAGACC; Reverse: TTTTTGGTTGAGCACAGG. The total RNA extraction from the HepG2 cells cultured one day after NPs adminstration was purified using the KingFisher Total RNA Kit and the KingFisher mL magnetic particle processors, both from Thermo Scientific (Vantaa, Finland). The concentration of cellular RNA was quantified by determining the absorbance maximum at the wavelength of 260 and 280 nm to optimum OD between 1.6 to 2.0 in a UV/Vis spectrometer (Lambda 40, PerkinElmer, Wellesley MA). Complementary DNA was obtained following a Deoxy+ real-time 2x SYBR green RT-PCR kit (Yeastern Biotech Co., Ltd., Taiwan) protocol. The real-time PCR was then performed in a PikoReal real-time PCR system (Thermo Scientific, Vantaa, Finland). Relative gene expression was determined using a ΔΔCq method[26] and normalized to a reference gene (GAPDH) and to a control (HepG2).

3. Results and discussion

Fig. 1 shows the characterization of MPIP NPs before the in vitro experiments. The DLS examination of NPs is a rapid process for measuring their size distribution and identifying their nanocomposite coating. Particle size distributions are shown in Fig. 1(a). The mean sizes of the magnetic nanoparticles, and peptide-imprinted nanoparticles (32 mol% ethylene) before and after template removal were 61±6, 241± 43 and 197± 12 nm, respectively; the size of the peptide-imprinted NPs decreased slightly to 189± 26.45 nm upon the rebinding of the peptide. Figure 1(b) displays the mean sizes of MPIP NPs that were prepared with various ethylene mol%. Interestingly, increasing ethylene content caused the mean size of the MPIP NPs to increase (from 207± 14 to 312± 29 nm, before template removal, for ethylene content from 27 to 44 mol%), but caused the size of the particles with rebound target to *shrink* slightly, from MPIPMPIP188± 41 to 147± 22 nm. Thus, rebinding target causes a much greater size contraction when the ethylene content is higher.

Preprints (www.preprints.org) | NOT PEER-REVIEWED | Posted: 29 September 2019 doi:10.20944/preprints201909.0324.v1

Peer-reviewed version available at Biomolecules 2019, 9, 651; doi:10.3390/biom9110651

Surface area measurements were made by the adsorption and desorption of nitrogen and BET analysis, as presented in Fig. 1(c). The lack of a knee in the curves reflects the extremely weak adsorbate-adsorbent interactions between MPIPs and nitrogen. The specific areas under the curves before and after the MPIPs were washed were 301.4±23.9, and 337.7± 35.4 m^2/g, respectively. The specific area after the MPIPs were washed was higher than before washing. The results reveal that target molecules (peptide A) were removed from the surface of MPIPs by washing, increasing their adsorption capacity. Figure 1(d) plots the magnetization curves of the MNP and PIP NPs before and after template removal. The saturated magnetization was approximately 52-56 emu/g, which may indicate that a few MNPs were present in a single MPIP NP. The removal of the template from the surface of NPs resulted in a small drop in magnetization. Figure 2 shows the adsorption peptides on the MPIP NPs. Figure 2(a) plots the capacities of MPIP and MNIP NPs that were prepared with various mol% of ethylene from 27 to 44. The highest rebinding capacity of MPIP NPs was achieved using EVAL that contained 32 mol% ethylene. The imprinting effectiveness is defined as the ratio of peptide adsorption on MPIP to that on MNIP, and is presented in Table 1. The imprinting effectiveness of MPIPs with EVAL that contained 32 mol% ethylene was 2.38, but other EVALs gave rather poor imprinting effectiveness, with nearly as much (or in one case, even more) peptide binding to non-imprinted controls as to imprinted NPs. MPIPs with 32 mol% ethylene were thus employed in the cellular experiments. Fig. 2(b) shows titrations of MPIPs and MNIPs (32 mol% ethylene) with peptide A.

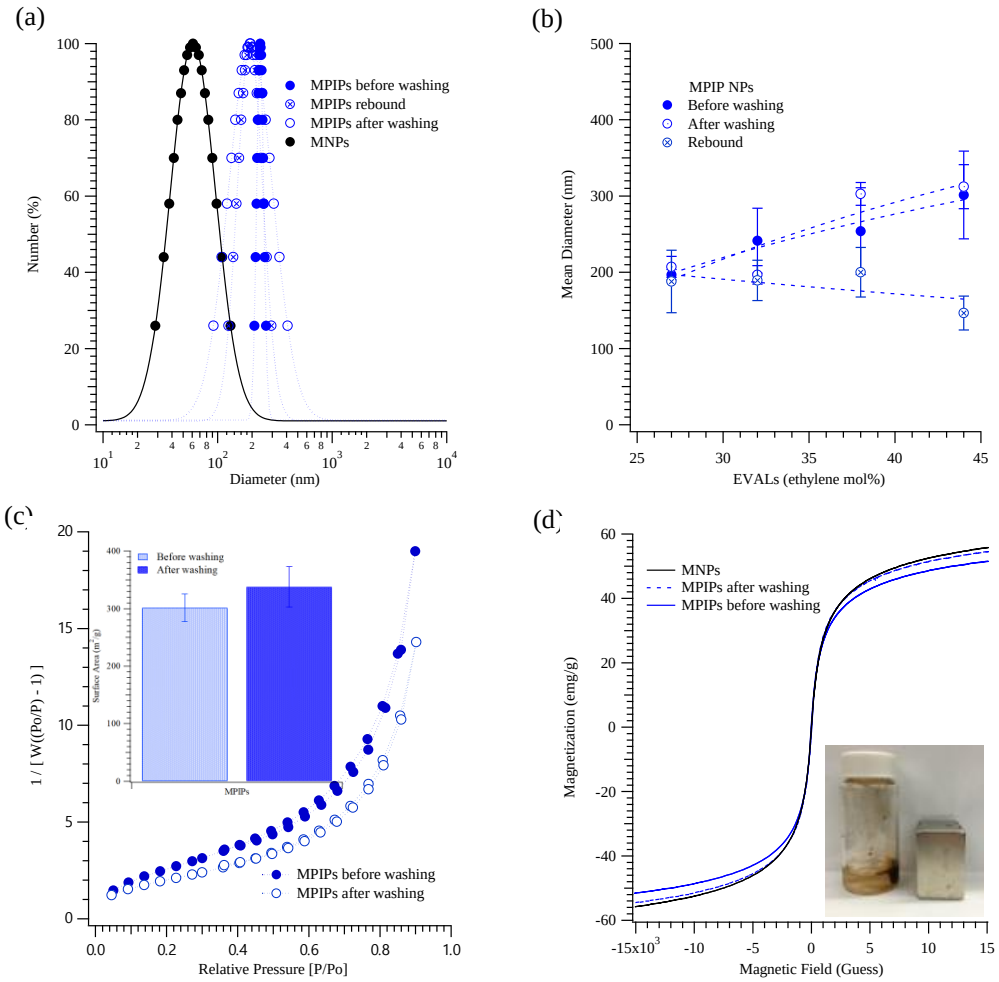

Figure 1. (a) Particles size distributions of MNPs (●); MPIPs before (●), after (○) template removal and rebound with template (⊕). (b) Mean diameters of MPIPs before (●), after (○) template removal and rebound with template (⊕) containing various ethylene mol% of EVAL. (c) Surface area of MPIPs before (●) and after (○) template removal measured by adsorption and desorption of nitrogen. (d)

Preprints (www.preprints.org) | NOT PEER-REVIEWED | Posted: 29 September 2019 doi:10.20944/preprints201909.0324.v1

Peer-reviewed version available at Biomolecules 2019, 9, 651; doi:10.3390/biom9110651

Magnetization of MNPs and MPIPs before and after template removal. Inset: MPIPs on the walls of a vial under magnetic field.

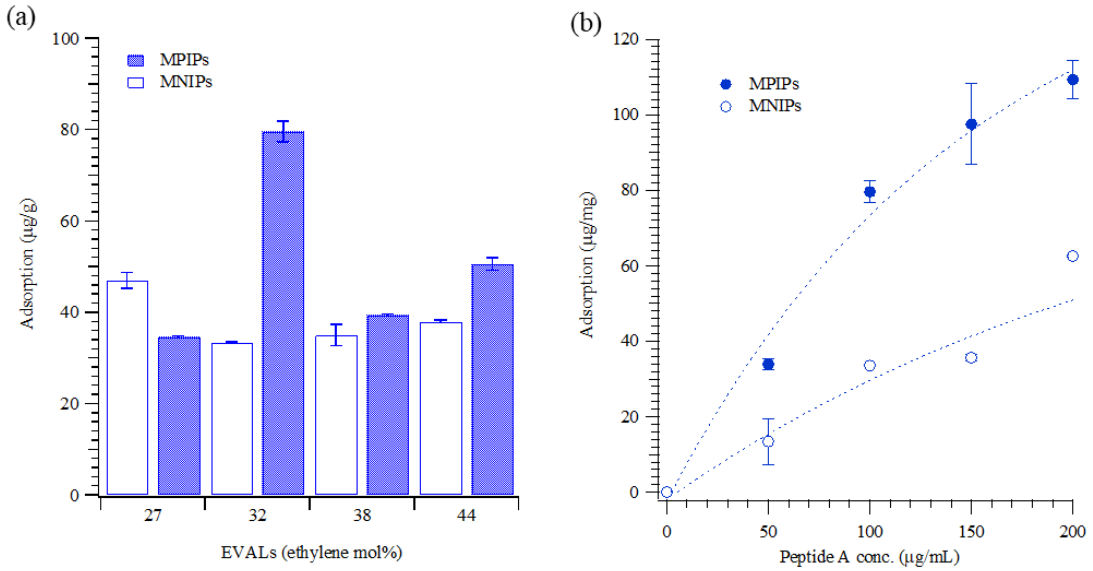

Figure 2. (a) Adsorption of peptide (100 µg/mL) on the MPIPs with imprinted onto various ethylene mol% of EVAL (b) Isothermal adsorption of MPIPs (●) and NIPs (○) with various of peptide concentrations.

Table 1. Prescreening of the binding of peptide molecules to magnetic peptide-imprinted and non-imprinted poly(ethylene-*co*-vinyl alcohol) nanoparticles. Imprinting effectiveness for four different ethylene mol-% are shown. Standard deviations are based on three individual measurements.

EVAL (ethylene mole %)	Peptide adsorption (g/g)		
	MPIPs	MNIPs	IF
27	34.62± 0.26	46.98± 1.78	0.74
32	**79.60± 2.27**	33.50± **0.14**	**2.38**
38	39.41± 0.24	35.03± 2.33	1.13
44	50.58± 1.39	37.99± 0.32	1.33

MPIPs: Magnetic peptide-imprinted polymers; MNIP: Magnetic non-imprinted polymers; IF: Imprinting effectiveness.

For the optimization of the ratio NK-92 to HepG2 cells, various cellular concentrations of NK-92 cells were added to HepG2 cells, and the viability of HepG2 cells was measured. The NK-92 cells were in suspension and grew mostly in clumps. In Fig. 3(a), 10^4 to 10^5 NK-92 cells were added to wells containing HepG2 cells. The viability of HepG2 was dramatically reduced, to approximately 40%, for the higher NK-92 numbers. The concentration of NK-92 cells in the human body is 2-72x10^4 cells/mL,[27] so 2x10^4 cells/well were used in the subsequent immunotherapy trials. The optical images in Fig. 4(a), *vide infra*, also confirmed that the concentrations of NK-92 cells increased from 1x10^4 to 10x10^4 cells/well. To compare the dosage of NPs to HepG2, various concentrations of NPs were added to HepG2 or MPIP NPs were added to NK-92 cells, and then the mixtures were added to HepG2 cells. In Fig. 3(b), the viabilities of HepG2 cells declined dramatically as a result of the activation the of NK-92 cells with MPIPs. Please note that zero particles also means zero NK-92 cells in Fig. 3(b). The most probable mechanistic explanation for this effect is that the PD-1 receptors on the surface of NK-92 cells were blocked by the binding of the MPIPs, causing the cellular viability of the MPIP NPs to be 20% lower than that of the MNIP NPs. Adding MPIP NPs to HepG2, followed by the addition of NK-92 cells, was not quite as effective as when the MPIP NPs were added to the NK-92 cells (presumably blocking them), and the activated cells were then added to the HepG2 cells. However, these results were still significantly better than obtained with MNIP controls, especially at concentrations higher

Preprints (www.preprints.org) | NOT PEER-REVIEWED | Posted: 29 September 2019 doi:10.20944/preprints201909.0324.v1

Peer-reviewed version available at Biomolecules 2019, 9, 651; doi:10.3390/biom9110651

than 200 g/mL. Figure 4(b) displays the SEM image of an HepG2 cell that was attacked by NK-92 cells, leaving fragments on its surface.

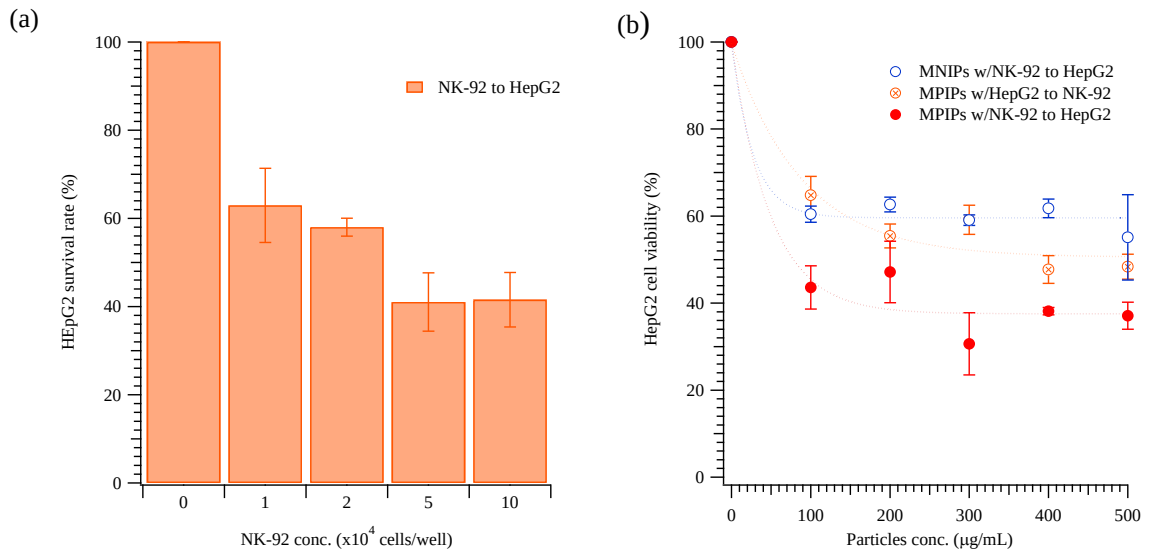

Figure 3. Cellular viability of HepG2 cells with various concentrations of (a) NK-92 cells, (b) MNIPs added with NK-92 cells (○), MPIPs incubated with HepG2 (⊕) and NK-92 cells (●) , MPIPs added with NK-92.

Preprints (www.preprints.org) | NOT PEER-REVIEWED | Posted: 29 September 2019 doi:10.20944/preprints201909.0324.v1

Peer-reviewed version available at Biomolecules 2019, 9, 651; doi:10.3390/biom9110651

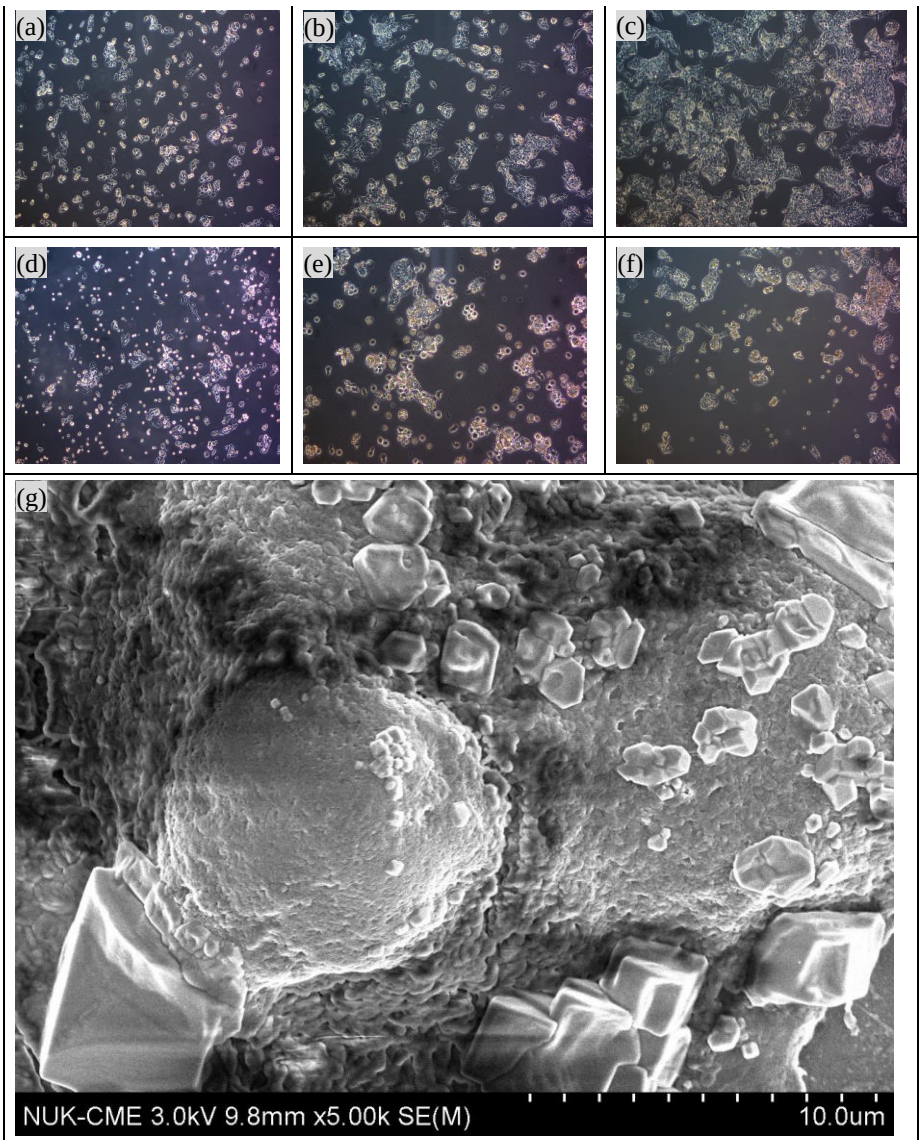

Figure 4. (a) Optical images of various concentrations of NK-92 cells added to HepG2 cells and (c) SEM image of a HepG2 with many NK-92 cells.

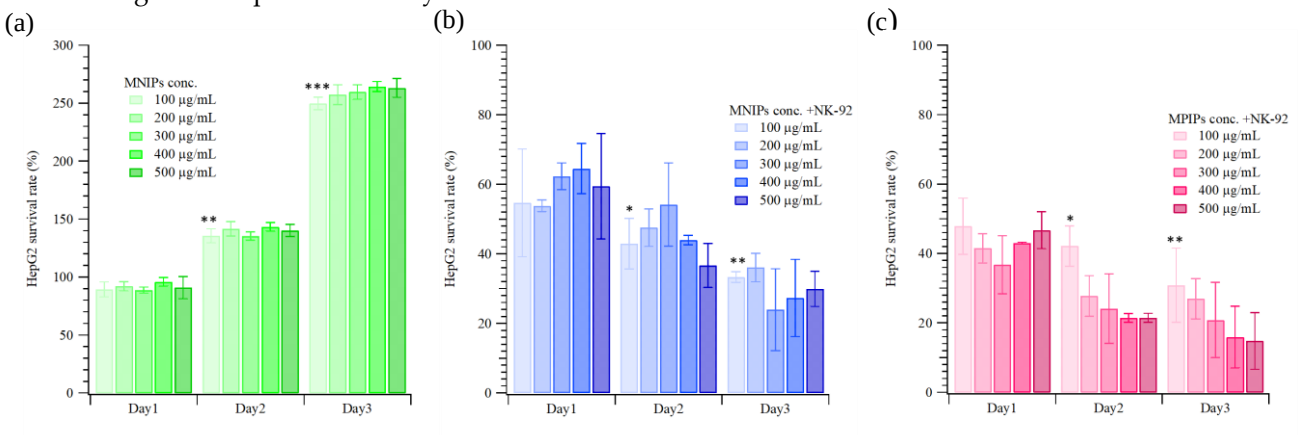

Figure 5. Continuous cellular viability measurements of HepG2 incubated with various concentrations of (a) MNIPs, (b) MNIPs added with NK-92 cells, (c) MPIPs added with NK-92 cells (*p<0.05; **p<0.005; ***p<0.0001 with respected to the same dosage treatment on day 1).

Figure 5 displays the results of treatment of HepG2 cells with nanocarriers and/or NK-92 cells (i.e. MNIPs, MNIPs or MPIPs with NK-92 cells). HepG2 cell samples were treated daily with specified concentrations of nanocarriers and/or NK-92 cells. In the presence of MNIPs without NK-92 cells,

Preprints (www.preprints.org) | NOT PEER-REVIEWED | Posted: 29 September 2019 doi:10.20944/preprints201909.0324.v1

Peer-reviewed version available at Biomolecules 2019, 9, 651; doi:10.3390/biom9110651

HepG2 cells proliferated well, with 2.5 times as many cells present after 3 days. As expected, treatment with MNIPs with NK-92 cells resulted in significant cell death, with only 24-36% of the cells remaining on day 3. Treatment with MPIPs and NK-92 cells was even more effective, with only 16-30% of the cells remaining on day 3, Figs. 5(b) and 5(c).

The apoptosis pathway of immunotherapy was enhanced with the additional PD-1 block of NK-92 cells to promote the expression of NK-κB and then caspase 8, caspase 3, as shown in Fig. 6. The surface protein Fas, an important effector of apoptosis, is a member of the death receptor family in the extrinsic death receptor pathway.[28] The Fas is activated by its natural ligand FasL.[29] Nuclear factor kappa B (NF-κB) activity is associated with various cellular events including proliferation, apoptosis, angiogenesis, chemo-radioresistance.[29] The expression of NF-κB1 in HepG2 cells was highest when MPIPs with NK-92 cells were added; the expression was much higher than with control MNIPs with NK-92 cells.

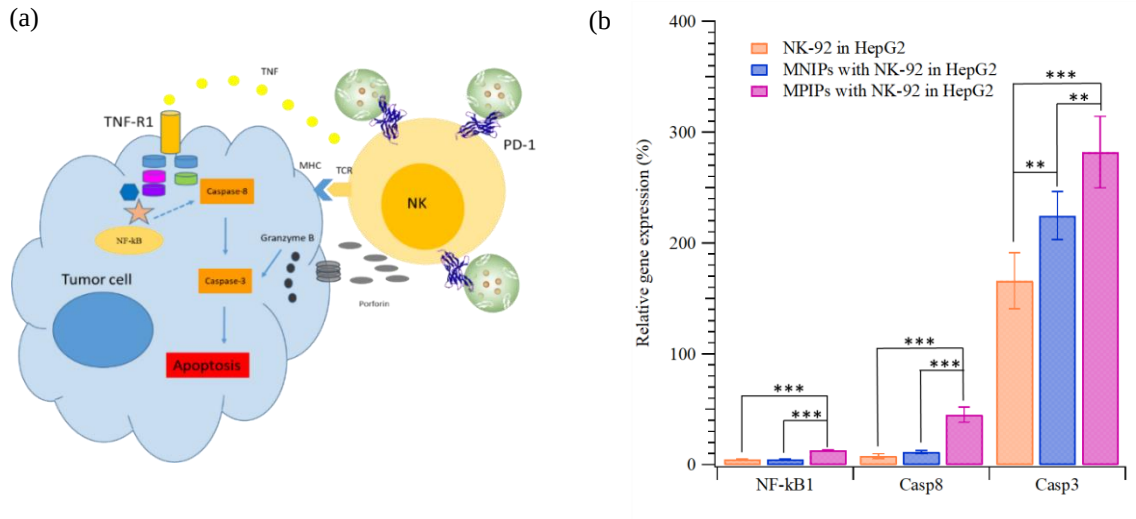

Figure 6. Relative gene expression of NK-kB1, Casp8, Casp3 of HepG2 cells when NK-92, NK-92 with MNIPs or NK-92 with MPIPs were added (*p<0.05, **p<0.005, and ***p<0.0001).

Preprints (www.preprints.org) | NOT PEER-REVIEWED | Posted: 29 September 2019 doi:10.20944/preprints201909.0324.v1

Peer-reviewed version available at Biomolecules 2019, 9, 651; doi:10.3390/biom9110651

The Fas-associated protein with death domain (FADD) induces the signaling complex, resulting in apoptotic cell death.[30] The pro-caspase-8 binds bound Fas-FADD to the activated Casp8,[29] leading to the activation of Casp3.[31] The increment of the NK- B for MPIPs from MNIPs or NK-92 cells only was about 10%, but that of Casp8 was about 40% from 10%. The expression of Casp3 was 1.7-, 2.2- and 2.8-fold of that on HepG2 cells with NK-92, and MNIPs or MPIPs. These results provide further support for the hypothesis that the binding of MPIPs with PD-1 protein of NK-92 is preventing the binding of PD-1 to PD-L1.

4. Conclusions

The imprinting of the peptide of PD-1 on MPIPs is of interest because of its potential to inhibit the self-tolerance of natural killer cells. We have synthesized molecularly imprinted nanoparticles, using a peptide derived from PD-1, and shown that these nanoparticles do significantly enhance the activity of natural killer cells toward HepG2 cells. A gene expression analysis revealed increased expression of NK- B, caspase 8 and especially caspase 3 in the HepG2 cells, especially when treated with NK-92 cells primed with the MPIPs. This work shows the potential of molecularly imprinted nanoparticles in immunotherapy, as natural killer checkpoint inhibitors.

Funding: This research was funded by Ministry of Science and Technology of ROC under Contract nos. MOST 106-2314-B-390-001-MY2 MOST 107-2923-M-390-001-MY3 and MOST 108-2314-B-214-005 -.

Conflicts of Interest: The authors declare no conflict of interest. The funders had no role in the design of the study; in the collection, analyses, or interpretation of data; in the writing of the manuscript, or in the decision to publish the results.

References

1. Ishida, Y.; Agata, Y.; Shibahara, K.; Honjo, T., Induced expression of PD-1, a novel member of the immunoglobulin gene superfamily, upon programmed cell death. *The EMBO journal* 1992, *11* (11), 3887-3895.

2. Moreno, B. H.; Ribas, A., Anti-programmed cell death protein-1/ligand-1 therapy in different cancers. *British journal of cancer* 2015, *112* (9), 1421.

3. Guan, J.; Lim, K. S.; Mekhail, T.; Chang, C.-C., Programmed death ligand-1 (PD-L1) expression in the programmed death receptor-1 (PD-1)/PD-L1 blockade: a key player against various cancers. *Archives of Pathology and Laboratory Medicine* 2017, *141* (6), 851-861.

4. Larkin, J.; Chiarion-Sileni, V.; Gonzalez, R.; Grob, J. J.; Cowey, C. L.; Lao, C. D.; Schadendorf, D.; Dummer, R.; Smylie, M.; Rutkowski, P., Combined nivolumab and ipilimumab or monotherapy in untreated melanoma. *New England journal of medicine* 2015, *373* (1), 23-34.

5. Das, R.; Verma, R.; Sznol, M.; Boddupalli, C. S.; Gettinger, S. N.; Kluger, H.; Callahan, M.; Wolchok, J. D.; Halaban, R.; Dhodapkar, M. V., Combination therapy with anti–CTLA-4 and anti–PD-1 leads to distinct immunologic changes in vivo. *The Journal of Immunology* 2015, *194* (3), 950-959.

6. Sim, H.-W.; Knox, J., Hepatocellular carcinoma in the era of immunotherapy. *Current problems in cancer* 2018, *42* (1), 40-48.

7. Prieto, J.; Melero, I.; Sangro, B., Immunological landscape and immunotherapy of hepatocellular carcinoma. *Nature reviews Gastroenterology & hepatology* 2015, *12* (12), 681.

8. Peng, H.; Jiang, X.; Chen, Y.; Sojka, D. K.; Wei, H.; Gao, X.; Sun, R.; Yokoyama, W. M.; Tian, Z., Liver-resident NK cells confer adaptive immunity in skin-contact inflammation. *The Journal of clinical investigation* 2013, *123* (4), 1444-1456.

Preprints (www.preprints.org) | NOT PEER-REVIEWED | Posted: 29 September 2019 doi:10.20944/preprints201909.0324.v1

Peer-reviewed version available at Biomolecules 2019, 9, 651; doi:10.3390/biom9110651

9. Peng, H.; Wisse, E.; Tian, Z., Liver natural killer cells: subsets and roles in liver immunity. *Cellular & molecular immunology* 2016, *13* (3), 328.

10. Vivier, E.; Tomasello, E.; Baratin, M.; Walzer, T.; Ugolini, S., Functions of natural killer cells. *Nature immunology* 2008, *9* (5), 503.

11. Hsu, J.; Hodgins, J. J.; Marathe, M.; Nicolai, C. J.; Bourgeois-Daigneault, M.-C.; Trevino, T. N.; Azimi, C. S.; Scheer, A. K.; Randolph, H. E.; Thompson, T. W., Contribution of NK cells to immunotherapy mediated by PD-1/PD-L1 blockade. *Journal of Clinical Investigation* 2018, *128* (10), 4654-4668.

12. Klingemann, H.; Boissel, L.; Toneguzzo, F., Natural killer cells for immunotherapy–advantages of the NK-92 cell line over blood NK cells. *Frontiers in immunology* 2016, *7*, 91.

13. Peer, D.; Karp, J. M.; Hong, S.; Farokhzad, O. C.; Margalit, R.; Langer, R., Nanocarriers as an emerging platform for cancer therapy. *Nature nanotechnology* 2007, *2* (12), 751.

14. Milling, L.; Zhang, Y.; Irvine, D. J., Delivering safer immunotherapies for cancer. *Advanced drug delivery reviews* 2017, *114*, 79-101.

15. Jo, S. D.; Nam, G.-H.; Kwak, G.; Yang, Y.; Kwon, I. C., Harnessing designed nanoparticles: current strategies and future perspectives in cancer immunotherapy. *Nano Today* 2017, *17*, 23-37.

16. Qian, H.; Liu, B.; Jiang, X., Application of nanomaterials in cancer immunotherapy. *Materials today chemistry* 2018, *7*, 53-64.

17. Ansell, R.; Ramström, O.; Mosbach, K., *Artificial antibodies prepared by molecular imprinting*. 1996; Vol. 42, p 1506-12.

18. Lee, M.-H.; Thomas, J. L.; Liao, C.-L.; Jurcevic, S.; Crnogorac-Jurcevic, T.; Lin, H.-Y., Polymers imprinted with three REG1B peptides for electrochemical determination of Regenerating Protein 1B, a urinary biomarker for pancreatic ductal adenocarcinoma. *Microchimica Acta* 2017, *184* (6), 1773-1780.

19. Lin, H.-Y.; Ho, M.-S.; Lee, M.-H., Instant formation of molecularly imprinted poly(ethylene-co-vinyl alcohol)/quantum dot composite nanoparticles and their use in one-pot urinalysis. *Biosensors and Bioelectronics* 2009, *25* (3), 579-586.

20. Lin, H.-Y.; Hsu, C.-Y.; Thomas, J. L.; Wang, S.-E.; Chen, H.-C.; Chou, T.-C., The microcontact imprinting of proteins: The effect of cross-linking monomers for lysozyme, ribonuclease A and myoglobin. *Biosensors and Bioelectronics* 2006, *22* (4), 534-543.

21. Bossi, A. M.; Sharma, P. S.; Montana, L.; Zoccatelli, G.; Laub, O.; Levi, R., Fingerprint-imprinted polymer: rational selection of peptide epitope templates for the determination of proteins by molecularly imprinted polymers. *Analytical chemistry* 2012, *84* (9), 4036-4041.

22. Lee, M.-H.; Thomas, J. L.; Liao, C.-L.; Jurcevic, S.; Crnogorac-Jurcevic, T.; Lin, H.-Y., Epitope recognition of peptide-imprinted polymers for Regenerating protein 1 (REG1). *Separation and Purification Technology* 2018, *192*, 213-219.

23. Lee, M.-H.; Thomas, J. L.; Ho, M.-H.; Yuan, C.; Lin, H.-Y., Synthesis of Magnetic Molecularly Imprinted Poly(ethylene-co-vinyl alcohol) Nanoparticles and Their Uses in the Extraction and Sensing of Target Molecules in Urine. *ACS Applied Materials & Interfaces* 2010, *2* (6), 1729-1736.

Preprints (www.preprints.org) | NOT PEER-REVIEWED | Posted: 29 September 2019 doi:10.20944/preprints201909.0324.v1

Peer-reviewed version available at Biomolecules 2019, 9, 651; doi:10.3390/biom9110651

24. Lee, M.-H.; Thomas, J. L.; Wang, H.-Y.; Chang, C.-C.; Lin, C.-C.; Lin, H.-Y., Extraction of resveratrol from polygonum cuspidatum with magnetic orcinol-imprinted poly(ethylene-co-vinyl alcohol) composite particles and their in vitro suppression of human osteogenic sarcoma (HOS) cell line. *Journal of Materials Chemistry* 2012, *22* (47), 24644-24651.

25. Lee, M.-H.; Thomas, J. L.; Chen, J.-Z.; Jan, J.-S.; Lin, H.-Y., Activation of tumor suppressor p53 gene expression by magnetic thymine-imprinted chitosan nanoparticles. *Chemical Communications* 2016, *52* (10), 2137-2140.

26. Pfaffl, M. W., A new mathematical model for relative quantification in real-time RT–PCR. *Nucleic acids research* 2001, *29* (9), e45-e45.

27. Wang, W.-n.; Zhou, G.-y.; Zhang, W.-l., NK-92 cell, another ideal carrier for chimeric antigen receptor. *Immunotherapy* 2017, *9* (9), 753-765.

28. Meteoglu, I.; Erdogdu, I. H.; Meydan, N.; Erkus, M.; Barutca, S., NF-KappaB expression correlates with apoptosis and angiogenesis in clear cell renal cell carcinoma tissues. *Journal of experimental & clinical cancer research : CR* 2008, *27* (1), 53-53.

29. Krammer, P. H.; Arnold, R.; Lavrik, I. N., Life and death in peripheral T cells. *Nature Reviews Immunology* 2007, *7*, 532.

30. Kischkel, F. C.; Hellbardt, S.; Behrmann, I.; Germer, M.; Pawlita, M.; Krammer, P. H.; Peter, M. E., Cytotoxicity-dependent APO-1 (Fas/CD95)-associated proteins form a death-inducing signaling complex (DISC) with the receptor. *The EMBO journal* 1995, *14* (22), 5579-5588.

31. Ashkenazi, A., Targeting the extrinsic apoptosis pathway in cancer. *Cytokine & Growth Factor Reviews* 2008, *19* (3), 325-331.